Designing flow regimes to support entire river ecosystems

Jonathan D. Tonkin[1,2]*, Julian D. Olden[3], David. M. Merritt[4], Lindsay V. Reynolds[4], Jane S. Rogosch[3], David A. Lytle[2]

[1] School of Biological Sciences, University of Canterbury, Christchurch 8140, New Zealand
[2] Department of Integrative Biology, Oregon State University, Corvallis, OR 97331, USA
[3] School of Aquatic and Fishery Sciences, University of Washington, Seattle, WA 98195, USA
[4] Watershed, Fisheries, Wildlife, Air and Rare Plants Staff and the National Stream and Aquatic Ecology Center, U.S.D.A. Forest Service, Fort Collins, Colorado 80526, USA
*Corresponding author: E: jonathan.tonkin@canterbury.ac.nz, Ph: +6433690413.

Abstract

Overcoming the physical limits of dam operations under nonstationarity will require creative approaches to flow management and modeling approaches that forecast the effects of management actions on multiple ecosystem components simultaneously. Using a novel multispecies modeling approach, we investigated the cross-ecosystem effects of environmental flow regimes designed for specific ecosystem outcomes. We reveal tradeoffs associated with flow regimes targeting riparian vegetation, fishes, and invertebrates. The different frequencies associated with each flow regime in some cases caused non-target ecosystem components to become locally extirpated within 50 years. By incorporating multiple flow frequencies, the natural flow regime enabled a balanced but sub-optimal response of the three ecosystem components (mean 72% of designer flow). Although returning to a natural flow regime may not be possible in highly managed rivers, novel flow regimes must incorporate diverse frequencies inherent to such a regime and accomodate the sometimes conflicting requirements of different taxa at different times.

Introduction

Dams and other types of human infrastructure have modified river hydrology globally and continue to do so at an unprecedented rate (Grill et al., 2019). Alteration of river flows comes at a major cost for the biota that inhabit freshwater and riparian (hereafter "river") ecosystems (Tonkin et al., 2018; Bunn and Arthington, 2002), threatening the countless ecosystem services they provide (Auerbach et al., 2014). Maintaining functional river ecosystems under uncertain hydroclimatic futures presents a major management challenge for both existing and planned dam projects (Tonkin et al., 2019; Palmer and Ruhi, 2019; Horne et al., 2019), requiring the consideration of flow prescriptions that target the health of downstream ecosystems (Acreman et al., 2014).

Environmental flows are increasingly used to help minimize the detrimental effects of dam management on river biota (Yarnell et al., 2015; Poff and Matthews, 2013). Designer environmental flows range from single events designed to achieve a specific goal, such as a flood for mobilizing sediment, to entire flow regimes designed to accommodate multiple ecosystem needs (Acreman et al., 2014). In practice, most environmental flow programs target a few important species or a particular component of the river ecosystem, such as recruitment of riparian vegetation or spawning of native fish (Olden et al., 2014) without directly considering secondary effects on other components of the ecosystem. This presents the question: Does flow management designed to benefit one important component of the river simultaneously protect other ecosystem components, or does it involve ecological tradeoffs that compromise other ecosystem components?

Calls for holistic ecosystem approaches to support sustainable riverine management continue to mount, yet robust quantitative models to underpin such efforts remain scarce (Poff and Olden, 2017). Here, we examined the responses to designer flows targeting three ubiquitous but distinct components of river ecosystems: riparian vegetation, fishes, and aquatic invertebrates. Using a mechanistic, multispecies modeling approach that links population dynamics and hydrology (WebTable 1), we designed flow regimes to maximize management outcomes for each of the three ecosystem components. The modeling approach permitted us to simultaneously design flows for a single ecosystem component as well as quantify the associated synergies or tradeoffs across other ecosystem components. These approaches enable an assessment of the potential ecological benefits or deficits of designer flow prescriptions at the ecosystem scale.

Methods

Management targets

Using species common to the Colorado River Basin of the southwestern United States, we defined management targets that natural resource managers often seek to maximize downstream from large dams. These outcomes relate to three components of a river-riparian (hereafter "river") ecosystem: cottonwood tree coverage as a percent of riparian carrying capacity, native fish species biomass as a percent of total carrying capacity (including nonnative fishes), and abundance of terrestrially-available benthic invertebrates (hereafter "aquatic invertebrates"). Cottonwood is an important native riparian tree that suffers from the effects of flow regime modification and competition with nonnatives such as tamarisk (Merritt and Poff, 2010). Native fish species are a focal management target because they face an uncertain future resulting from altered hydrology and impacts from nonnative species (Chen and Olden, 2017). Terrestrially-available aquatic invertebrates serve as aquatic prey for fish and, upon emergence as winged adults, as terrestrial prey for birds, bats, lizards and other riparian animals (Baxter et al., 2005). Using these targets, coupled with mechanistic population models, we identified flow regimes that maximized the value of each ecosystem component and explored tradeoffs in achieving positive outcomes across all three components by projecting the flow time-series for up to 200 years into the future. We also examined a natural flow regime scenario using a hydrograph derived from a large free-flowing river supporting riparian vegetation, fish and aquatic invertebrate assets (upper Verde River, Arizona, USA) and quantified the community-wide population responses across ecosystem components (Fig. 1). Detailed methods are presented in WebPanel 1.

Modeling frameworks

We modeled the three ecosystem components using three independent existing models parameterized using empirical data. Riparian vegetation and fishes were modeled using a novel application of coupled, stage-structured matrix population models projected at annual time steps (Lytle et al., 2017; Rogosch et al., 2019). Informed by empirical data from a variety of sources, these models link the flow regime directly with population dynamics in a coupled framework that enables an understanding of whole-community dynamics and can incorporate stochasticity by taking random draws from a sequence of river flow year types. Floods and droughts interact with vital rates, affecting population sizes, which opens vacant space (vegetation) or biomass (fish) for recruitment during the next year if conditions are met. Both models have demonstrated a strong ability to recover known patterns on the landscape via tests against empirical data (Lytle et al., 2017; Rogosch et al., 2019).

The plant community comprised five taxa with six stage classes from seedling to reproductive adult: cottonwoods (*Populus deltoides*), tamarisk (*Tamarix ramosissima*), willow (*Salix exigua*), meadow grasses, and sagebrush (*Artemisia tridentata*). These taxa are representative of dominant groups across dryland regions. The fish community comprised three native species to the southwest USA (each with three stage classes): desert sucker (*Catostomus clarki*; CACL), Sonora sucker (*Catostomus insignis*; CAIN) and roundtail chub (*Gila robusta*; GIRO); and four non-native species (each with three stage classes): yellow bullhead (*Ameiurus natalis*; AMNA), green sunfish (*Lepomis cyanellus*; LECY), smallmouth bass (*Micropterus dolomieu*; MIDO), and red shiner (*Cyprinella lutrensis*; CYLU).

Benthic invertebrates, which experience population dynamics at intra-annual timescales, were modeled using a novel form of the continuous logistic growth model that enables carrying capacity (K) to fluctuate through time (McMullen et al., 2017). Carrying capacity, in this case, responds to flood events. For flood-adapted species, carrying capacity is highest immediately post-flood. The magnitude of a flood pulse determines the magnitude of change in K, and this relationship can be modeled for events of any magnitude and for multiple, repeated events. Contrary to the fish and riparian plant models, this model operates on individual populations in that the populations do not share a finite resource such as space or biomass: each population has its own carrying capacity. We modeled three invertebrate taxa: a fast life-cycle, flood-adapted mayfly, *Fallceon* spp. (Ephemeroptera: Baetidae); a slow life-cycle, flood-adapted dragonfly *Progomphus* spp. (Odonata: Gomphidae); and a flood-averse ostracod seed shrimp (Crustacea: Ostracoda) (see WebPanel 1).

Vital rates for all species included in the models were obtained from independent sources in the literature and from field studies (see WebPanel 1 for details). Vital rates included stage-specific mortality rates in response to flow events for fish and riparian plants, and population growth rates and flow-specific mortality rates for aquatic invertebrates.

Hydrograph details

Although our approach was simulation-based (with parameterizations from field data) in a generalized river in the southwestern United States, we used a real flow regime to generate a natural hydrograph vector. To do this, we sourced a 45-year (1964-2008) historical hydrograph from the upper Verde River (USGS gauge number 09503700) near Paulden, Arizona. All three groups were modeled from this one central flow regime in our natural flow regime scenario, enabling a comparison of community dynamics across the whole ecosystem. For details of conversion of the hydrograph for each model, see WebPanel 1.

Flow design

We searched flow parameter space for optimal sequences of flow events that maximized each of the management targets associated with riparian plants, native fishes, and aquatic invertebrates. For riparian plants and fishes, this search for an optimal flow design followed a series of steps that incrementally adjusted the frequency of particular year-types. The resulting prescribed flow regime for riparian vegetation consisted of a spring flood every six years, preceded by a drought year, with a series of non-event years in between (WebTable 1). These floods occurred within the spring window that enabled cottonwood and tamarisk to recruit (synchronized with seed release). The resulting prescribed flow regime for native fish percentage consisted of a spring flood every year. In contrast to the plant and fish models, the invertebrate models operates in continuous time. Because the aquatic invertebrates we modeled do not compete directly with each other for a resource such as space or food, we modelled the the three taxa independently so that each species had its own carrying capacity, which we scaled to 100. We sought to maximize the average value of the two terrestrially-available target taxa (i.e. % of K) over the 20-year evaluation period. The resulting scenario that maximized the target was four small pulses per year, below the threshold of a flood in either the fish or riparian models. Therefore, the invertebrate prescription results in 100% of years being non-event years for the non-target taxa.

Results and discussion

We identified specific flow regimes that were highly beneficial to populations of each targeted ecosystem component—cottonwoods, native fishes, and aquatic invertebrates—by maximizing their average population sizes through time (Fig. 1 - 2, WebFigure 1 - 3). These designer flow regimes, optimized separately for each ecosystem target, always outperformed the historical natural regime for the intended ecosystem component, suggesting that artificially-imposed flow regimes can in some instances generate greater population sizes than the natural flow

regime. This finding is consistent with recent studies targeting native fish abundance in the San Juan River, United States, and fisheries yield in the Mekong River Basin (Sabo et al., 2017; Chen and Olden, 2017).

However, our results highlight that a narrow management focus on a single taxonomic group, as is commonly the case for environmental flow efforts, may come at a cost for other components of the ecosystem (Fig. 3, WebFigure 4). Each scenario had at least one major losing ecosystem component: cottonwoods declined in the fish-prescribed flows (7% of natural flow $\%K$), native fish abundance declined in the vegetation-prescribed flows (5% of natural flow $\%K$), and both vegetation (10% of natural flow $\%K$) and native fishes (6% of natural flow $\%K$) declined in the invertebrate-prescribed flows. Thus, major ecological deficits appear to accompany environmental flow regimes that target a single ecosystem outcome.

Each designer flow regime had a characteristic temporal frequency, reflecting the varying biology of the three ecosystem components: approximately decadal or half-decadal timescale flow events for riparian vegetation, annual or near-annual for fishes, and intra-annual for invertebrates (Fig. 1 - 2, WebTable 1). Cottonwood thrive under regimes with large recruitment floods approximately every six years followed by growth years (i.e. non-event years), with a drought year included to limit population growth of drought-intolerant competitor species (Lytle et al., 2017). Native fishes prosper under flow regimes with more frequent and reliable (i.e. annual) spawning floods and no drought (Rogosch et al., 2019). Thus, bigger floods are beneficial for vegetation and fishes, but the timescale of response differs. By contrast, the pulses required for maintaining aquatic invertebrates are insufficiently large to exert a positive benefit for native fishes or cottonwood; this taxonomic group responds best to flow regimes comprising many regular small pulses to maintain shallow riffle habitat. Without regular small pulses (larger pulses may also be incorporated), slower-water specialist invertebrates, many of which do not have a terrestrial lifecycle phase, become dominant (McMullen et al., 2017). In summary, various temporal frequencies are thus fundamental aspects of a flow regime designed for the benefit of an entire ecosystem—a characteristic of the historical natural flow regime that is essential for the vitality of rivers (Fig. 1) (Poff et al., 1997; Naiman et al., 2008; Tonkin et al., 2019). Administering such ecosystem-level designer flows may be challenging if single sensitive (threatened, endangered, or red listed) species provide the impetus (legal mandate) for implementation of designer flows.

Contrary to the designer flow regimes, the natural flow regime scenario resulted in species persistence for all ecosystem components, although population sizes were never as large as those achievable under designer flow regimes (vegetation: 66% of designer flow; fishes: 77%; invertebrates: 72%) (Fig. 2). We attribute this to the fact that most natural flow regimes exhibit an array of hydrologic events at multiple temporal frequencies (from intra-annual to inter-decadal), thereby satisfying the ecological needs of diverse biological groups with sometimes conflicting requirements (Fig. 1 - 2). Most dam operations fail to provide this

diverse portfolio of flows that are important for recruitment, migration, spawning and juvenile rearing across a broad array of taxa (Palmer and Ruhi, 2019). Organisms have evolved life histories to capitalize on natural cycles of flooding and drought (Lytle and Poff, 2004). However, the evolutionary fine-tuning, and potential for rapid evolution, of entire ecosystems to the natural flow regime remains an important topic of inquiry, as does the interaction among the different ecosystem components that we have yet to consider (e.g. invertebrates are a food source for fish, plants provide organic matter for invertebrates). Maintaining these cycles is fundamental to the maintenance of diverse and resilient communities into the future (Tonkin et al., 2018). Flooding also plays a critical role in maintaining functional river geomorphology by creating and maintaining critical off-channel habitats, and mobilizing sediment, woody debris and essential nutrients (Yarnell et al., 2015). Whether maintaining such variability is possible with environmental flows remains to be seen given the rapidly shifting state of river flows worldwide (Poff, 2018; Poff and Olden, 2017; Tonkin et al., 2019).

Interannual variability in flows that are supported by natural flow regimes enables the persistence of multiple species across diverse taxonomies (Fig. 2). Simply put, some flows benefit particular suites of species in certain years to the detriment of others, but gains made during these periods enable their persistence and coexistence with other species, often through unfavorable periods, over long time-scales (Tonkin et al., 2017; Ruhí et al., 2016). Through time, the full dynamism of river hydrology accommodates higher temporal diversity, emphasizing the importance of taking a functional whole-regime approach to designing and prescribing environmental flows (Yarnell et al., 2015). In long-lived species, such as riparian vegetation, desired outcomes may only manifest in response to flow prescriptions that operate over multiple years or decades. Bottomline: plants and animals are committed to long-term flow regimes; humans similarly need to be committed to long-term flow management.

The mechanisms that produced undesired non-target outcomes were specific to each ecosystem component. For fishes, native species were forecast to become locally extirpated within approximately 50 years due to a complete lack of flood recruitment events reflected in the invertebrate flow prescription, and or a combination of droughts with too-infrequent flood events reflected in the riparian flow prescription, both of which allowed non-native fishes to dominate the community (Fig. 2, WebFigure 2). This finding is supported by empirical research in the American Southwest (Chen and Olden, 2017; Ruhí et al., 2016; Rogosch et al., 2019). Cottonwoods collapsed in response to native fish-prescribed flows due to phreatophytic, flood-tolerant willow species dominating at high flood frequencies. In response to a lack of recruitment flood events under the invertebrate flow prescription, cottonwoods were replaced by non-riparian upland species such as sagebrush (Fig. 2, WebFigure 1), representing a loss of riparian trees and shrubs that comprise essential and high quality habitat for diverse terrestrial fauna (Merritt and Bateman, 2012). The target invertebrates exhibited much greater fluctuations in population abundance than fish or vegetation (Fig. 2, WebFigure 3). Both the

fish and riparian prescriptions did not meet the needs of the aquatic invertebrates due to a lack of regularly-spaced pulses required to maintain open habitat for the two target taxa: a flood-resilient mayfly *Fallceon* spp. (Ephemeroptera: Baetidae), and a flood-resistant dragonfly *Progomphus* spp. (Odonata: Gomphidae) (McMullen et al., 2017). These clear tradeoffs reflect situations where flows are targeted not for an entire community response (e.g. community evenness), but a specific component of each community. Different outcomes may be apparent with alternative ecological targets, but the important implication of this research is that narrowly targeting individual ecological outcomes with specific flows may have broader ecosystem-wide negative impacts.

Different frequencies of response to flows among taxa presents unique challenges when setting out to optimally manage rivers in an environmental flows context. Experimental flood programs have in some cases demonstrated benefits to non-target ecosystem components (e.g. River Spöl, Switzerland: Robinson et al. (2018); Bill Williams River, USA: Shafroth et al. (2010)). However, the potential ecosystem-wide impacts of narrowly prescribed flow regimes emphasizes the need to consider entire ecosystems as the ultimate management goal, rather than focus on single physical (e.g. sediment) or biological (e.g. fish) outcomes (Olden et al., 2014). Considering whole-ecosystem integrity will inevitably require mimicking some functional components of natural hydrologic variability (Yarnell et al., 2015), most notably the presence of multiple frequencies and magnitudes of flow events over extended timescales. However, hydroclimatic nonstationarity, where the envelope of variability in which a river flow regime fluctuates no longer remains fixed (Milly et al., 2008), means returning to the inherently dynamic natural flow regime as a management target may no longer be the most beneficial option (Poff, 2018; Acreman et al., 2014; Tonkin et al., 2019). Overcoming the physical limits of dam operations under nonstationarity, therefore, requires creative approaches to flow management (Poff and Olden, 2017) and a coherent modeling approach that forecasts the effects of management actions on multiple ecosystem components simultaneously.

The unprecedented magnitude at which river flows are being altered across the developing world, combined with the already large proportion of dammed rivers in the developed world, puts into question the long-term sustainability of freshwater ecosystems (Poff and Matthews, 2013; Grill et al., 2019). Environmental flow regimes targeting single ecological outcomes may help to alleviate some of these detrimental effects, but we urge caution in their application due to the potential of unintended collateral impacts on other components of the ecosystem. How can entire ecosystems be better considered in modern day flow management strategies? We assert that designing flows for the benefit of entire ecosystems requires long-term perspectives that embrace hydrologic dynamism involving critical flow events that occur at multiple temporal frequencies. While returning to the historical natural flow regime is an increasingly distant option in highly managed rivers in a nonstationary world (Tonkin et al., 2019), environmental flows must remain founded on the principles of the natural flow

regime paradigm.

Acknowledgements

Funding was provided in part by the US Department of Defense (SERDP RC-2511) and the US Department of Agriculture Forest Service. JDT is supported by a Rutherford Discovery Fellowship administered by the Royal Society Te Apārangi (RDF-18-UOC-007).

References

Acreman, M., A. H. Arthington, M. J. Colloff, C. Couch, N. D. Crossman, F. Dyer, I. Overton, C. A. Pollino, M. J. Stewardson, and W. Young. 2014. Environmental flows for natural, hybrid, and novel riverine ecosystems in a changing world. Frontiers in Ecology and the Environment, **12**:466–473.

Anderson, K. E., A. J. Paul, E. McCauley, L. J. Jackson, J. R. Post, and R. M. Nisbet. 2006. Instream flow needs in streams and rivers: the importance of understanding ecological dynamics. Frontiers in Ecology and the Environment, **4**:309–318.

Auerbach, D. A., D. B. Deisenroth, R. R. McShane, K. E. McCluney, and N. L. Poff. 2014. Beyond the concrete: Accounting for ecosystem services from free-flowing rivers. Ecosystem Services, **10**:1–5.

Baxter, C. V., K. D. Fausch, and W. Carl Saunders. 2005. Tangled webs: Reciprocal flows of invertebrate prey link streams and riparian zones. Freshwater Biology, **50**:201–220.

Bunn, S. E. and A. H. Arthington. 2002. Basic principles and ecological consequences of altered flow regimes for aquatic biodiversity. Environmental Management, **30**:492–507.

Caswell, H. 2001. Matrix Population Models: Construction, Analysis, and Interpretation. Sinauer Associates, Inc., Sunderland, MA, USA.

Chen, W. and J. D. Olden. 2017. Designing flows to resolve human and environmental water needs in a dam-regulated river. Nature Communications, **8**:2158.

Cooper, D. J., D. M. Merritt, D. C. Andersen, and R. A. Chimner. 1999. Factors controlling the establishment of fremont cottonwood seedlings on the upper Green River, USA. Regulated Rivers: Research & Management, **15**:419–440.

Grill, G., B. Lehner, M. Thieme, B. Geenen, D. Tickner, F. Antonelli, S. Babu, P. Borrelli, L. Cheng, H. Crochetiere, H. E. Macedo, R. Filgueiras, M. Goichot, J. Higgins, Z. Hogan,

B. Lip, M. E. McClain, J. Meng, M. Mulligan, C. Nilsson, J. D. Olden, J. J. Opperman, P. Petry, C. R. Liermann, L. Sáenz, S. Salinas-Rodríguez, P. Schelle, R. J. P. Schmitt, J. Snider, F. Tan, K. Tockner, P. H. Valdujo, A. van Soesbergen, and C. Zarfl. 2019. Mapping the world's free-flowing rivers. Nature, **569**:215–221.

Horne, A. C., R. Nathan, N. L. Poff, N. R. Bond, J. A. Webb, J. Wang, and A. John. 2019. Modeling flow-ecology responses in the anthropocene: Challenges for sustainable riverine management. BioScience, **nil**:nil.

Lytle, D., D. Merritt, J. Tonkin, J. Olden, and L. Reynolds. 2017. Linking river flow regimes to riparian plant guilds: A community-wide modeling approach. Ecological Applications, **27**:1338–1350.

Lytle, D. A. and N. Poff. 2004. Adaptation to natural flow regimes. Trends in Ecology & Evolution, **19**:94–100.

Mahoney, J. M. and S. B. Rood. 1998. Streamflow requirements for cottonwood seedling recruitment – an integrative model. Wetlands, **18**:634–645.

McMullen, L., P. De Leenheer, J. Tonkin, and D. Lytle. 2017. High mortality and enhanced recovery: Modelling the countervailing effects of disturbance on population dynamics. Ecology Letters, **20**:1566–1575.

Merritt, D. M. and H. L. Bateman. 2012. Linking stream flow and groundwater to avian habitat in a desert riparian system. Ecological Applications, **22**:1973–1988.

Merritt, D. M. and N. L. R. Poff. 2010. Shifting dominance of riparian *Populus* and *Tamarix* along gradients of flow alteration in western North American rivers. Ecological Applications, **20**:135–152.

Milly, P. C. D., J. Betancourt, M. Falkenmark, R. M. Hirsch, Z. W. Kundzewicz, D. P. Lettenmaier, and R. J. Stouffer. 2008. Stationarity is dead: Whither water management? Science, **319**:573–574.

Naiman, R. J., J. J. Latterell, N. E. Pettit, and J. D. Olden. 2008. Flow variability and the biophysical vitality of river systems. Comptes Rendus Geoscience, **340**:629–643.

Olden, J. D., C. P. Konrad, T. S. Melis, M. J. Kennard, M. C. Freeman, M. C. Mims, E. N. Bray, K. B. Gido, N. P. Hemphill, D. A. Lytle, L. E. McMullen, M. Pyron, C. T. Robinson, J. C. Schmidt, and J. G. Williams. 2014. Are large-scale flow experiments informing the science and management of freshwater ecosystems? Frontiers in Ecology and the Environment, **12**:176–185.

Olden, J. D., N. L. Poff, and K. R. Bestgen. 2006. Life-history strategies predict fish invasions and extirpations in the Colorado River Basin. Ecological Monographs, **76**:25–40.

Palmer, M. and A. Ruhi. 2019. Linkages between flow regime, biota, and ecosystem processes: Implications for river restoration. Science, **365**:eaaw2087.

Poff, N. L. 2018. Beyond the natural flow regime? Broadening the hydro-ecological foundation to meet environmental flows challenges in a non-stationary world. Freshwater Biology, **63**:1011–1021.

Poff, N. L., J. D. Allan, M. B. Bain, J. R. Karr, K. L. Prestegaard, B. D. Richter, R. E. Sparks, and J. C. Stromberg. 1997. The natural flow regime. BioScience, **47**:769–784.

Poff, N. L. and J. H. Matthews. 2013. Environmental flows in the anthropocence: Past progress and future prospects. Current Opinion in Environmental Sustainability, **5**:667–675.

Poff, N. L. and J. D. Olden. 2017. Can dams be designed for sustainability? Science, **358**:1252–1253.

R Core Team. 2017. R: A Language and Environment for Statistical Computing. R Foundation for Statistical Computing, Vienna, Austria.

Robinson, C. T., A. R. Siebers, and J. Ortlepp. 2018. Long-term ecological responses of the River Spöl to experimental floods. Freshwater Science, **37**:433–447.

Rogosch, J., J. Tonkin, D. Lytle, D. Merritt, L. Reynolds, and J. Olden. 2019. Increasing drought favors nonnative fishes in a dryland river: Evidence from a multispecies demographic model. Ecosphere, **10**:e02681.

Ruhí, A., J. D. Olden, and J. L. Sabo. 2016. Declining streamflow induces collapse and replacement of native fish in the american southwest. Frontiers in Ecology and the Environment, **14**:465–472.

Sabo, J. L., A. Ruhi, G. W. Holtgrieve, V. Elliott, M. E. Arias, P. B. Ngor, T. A. Räsänen, and S. Nam. 2017. Designing river flows to improve food security futures in the Lower Mekong Basin. Science, **358**:eaao1053.

Shafroth, P. B., A. C. Wilcox, D. A. Lytle, J. T. Hickey, D. C. Andersen, V. B. Beauchamp, A. Hautzinger, L. E. McMullen, and A. Warner. 2010. Ecosystem effects of environmental flows: Modelling and experimental floods in a dryland river. Freshwater Biology, **55**:68–85.

Tonkin, J., M. Bogan, N. Bonada, B. Rios-Touma, and D. Lytle. 2017. Seasonality and predictability shape temporal species diversity. Ecology, **98**:1201–1216.

Tonkin, J., D. Merritt, J. Olden, L. Reynolds, and D. Lytle. 2018. Flow regime alteration degrades ecological networks in riparian ecosystems. Nature Ecology and Evolution, **2**:86–93.

Tonkin, J., N. Poff, N. Bond, A. Horne, D. Merritt, L. Reynolds, J. Olden, A. Ruhi, and D. Lytle. 2019. Prepare river ecosystems for an uncertain future. Nature, **570**:301–303.

Yarnell, S. M., G. E. Petts, J. C. Schmidt, A. A. Whipple, E. E. Beller, C. N. Dahm, P. Goodwin, and J. H. Viers. 2015. Functional flows in modified riverscapes: Hydrographs, habitats and opportunities. BioScience, **65**:963–972.

Figure legends

Figure 1: The modeled ecosystem components and flow regimes. A. The three ecosystem components examined: riparian plants (target: % cottonwoods), fish (target: % native species), and benthic invertebrates (target: % terrestrially-available taxa). B. A schematic of the three flow regimes designed for each target ecosystem component. The plant and fish models are based on year-types and the invertebrate model responds to individual flow events, thus the 'hydrographs' are for visual purposes only (e.g. the plant prescription shows a single large flood event every 6 years, preceded by a drought year). The bottom panel represents the historical hydrograph taken from the Verde River, Arizona, USA. Note the logarithmic scale on the y-axis.

Figure 2: Results of simulations for target and non-target taxa, both within and among ecosystem components. Target taxa (plants: % cottonwood; fish: % native species; invertebrates: % terrestrially-available taxa) are shown as the colored lines and non-target taxa as grey. For plants, the four grey lines represent the four non-target plant taxa individually. For fish, the single grey line represents the four non-native fish species combined (the band around the line represents 2 standard errors around the mean of 100 iterations). For invertebrates, the grey line represents the non-target taxa (ostracods). See Supporting Information for full results. Model evaluation (e.g. Fig. 3) discarded the first ten years as a burn-in period.

Figure 3: The ecosystem-wide effects of designer and natural flow regimes. Each of the four figure sectors represents a particular flow regime and/or ecosystem component: the natural flow regime and three designer flow regimes (riparian vegetation, fishes, and invertebrates). The effects of designer flow regimes on each component are shown, both targeted (arrow returns to same figure sector; e.g. fish to fish) and non-targeted (arrow from one sector to another; e.g. fish to plants), as well as the natural flow regime. Arrow widths correspond to the relative effects of a particular flow scenario (source of arrow) on all other components (arrow endpoint; larger equal more positive responses). These values are shown as proportions of maximum in the outermost bars (1 = maximum; e.g. native fish biomass 100% of carrying capacity). For instance, when designing flows to most benefit native fishes, fish respond strongly (large arrow and outer bar) but plants perform poorly (small arrow and bar). The bar tracking the circumference of the center arrows represents the difference between the natural and prescribed flow for the group in that sector (given in percentage). For example, under the natural flow regime, fish achieve 77% of the biomass achieved under the designer flow.

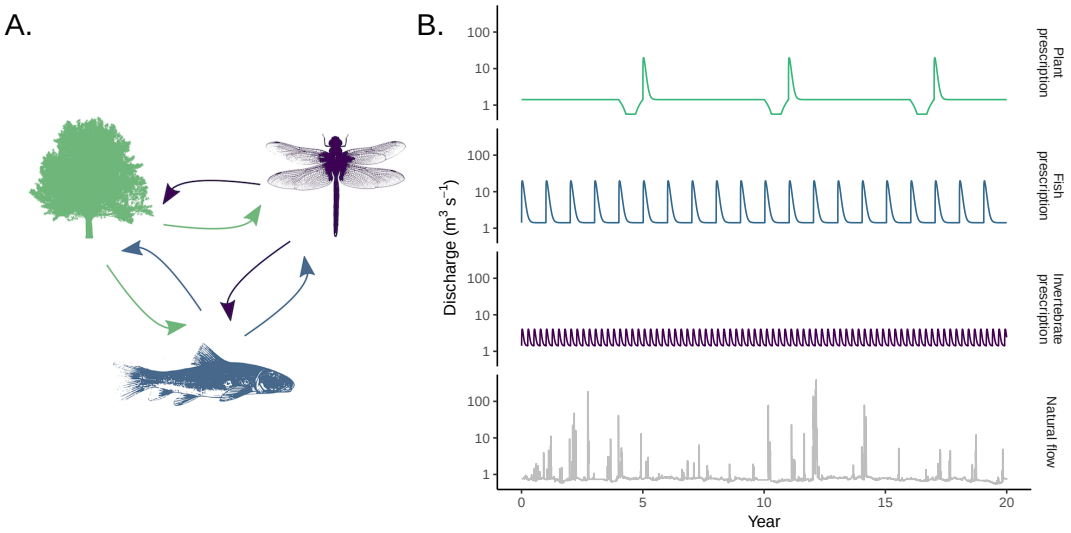

Figure 1: The modeled ecosystem components and flow regimes. A. The three ecosystem components examined: riparian plants (target: % cottonwoods), fish (target: % native species), and benthic invertebrates (target: % terrestrially-available taxa). B. A schematic of the three flow regimes designed for each target ecosystem component. The plant and fish models are based on year-types and the invertebrate model responds to individual flow events, thus the 'hydrographs' are for visual purposes only (e.g. the plant prescription shows a single large flood event every 6 years, preceded by a drought year). The bottom panel represents the historical hydrograph taken from the Verde River, Arizona, USA. Note the logarithmic scale on the y-axis.

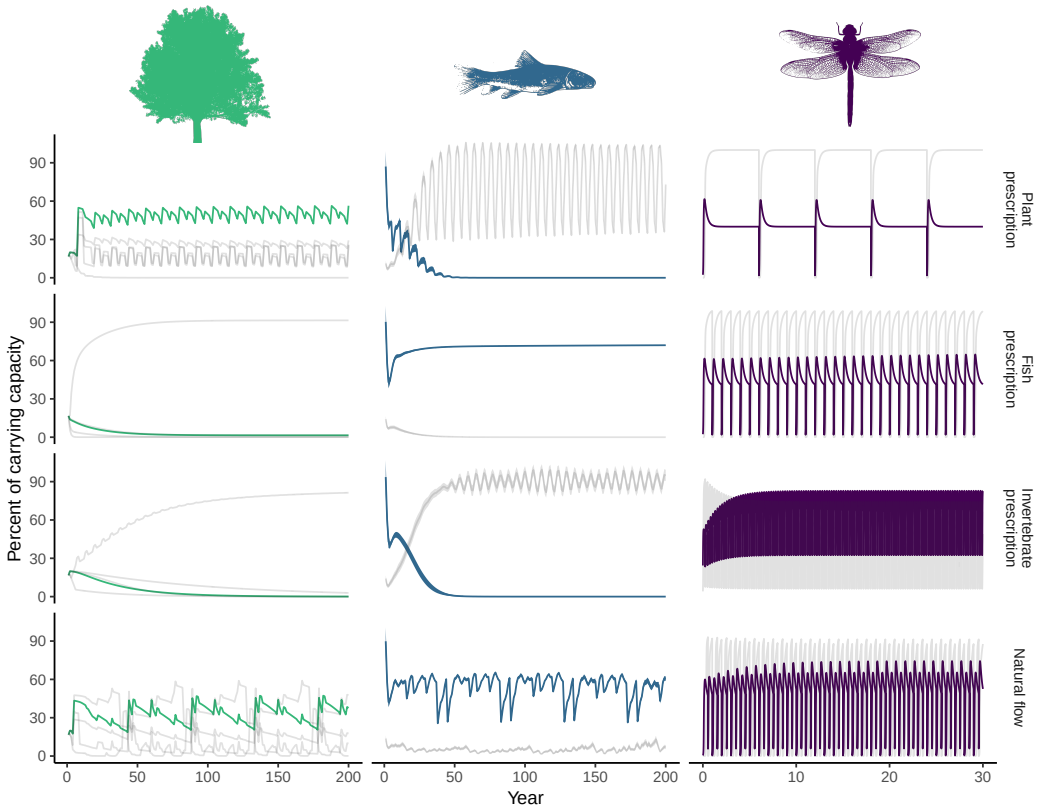

Figure 2: Results of simulations for target and non-target taxa, both within and among ecosystem components. Target taxa (plants: % cottonwood; fish: % native species; invertebrates: % terrestrially-available taxa) are shown as the colored lines and non-target taxa as grey. For plants, the four grey lines represent the four non-target plant taxa individually. For fish, the single grey line represents the four non-native fish species combined (the band around the line represents 2 standard errors around the mean of 100 iterations). For invertebrates, the grey line represents the non-target taxa (ostracods). See Supporting Information for full results. Model evaluation (e.g. Fig. 3) discarded the first ten years as a burn-in period.

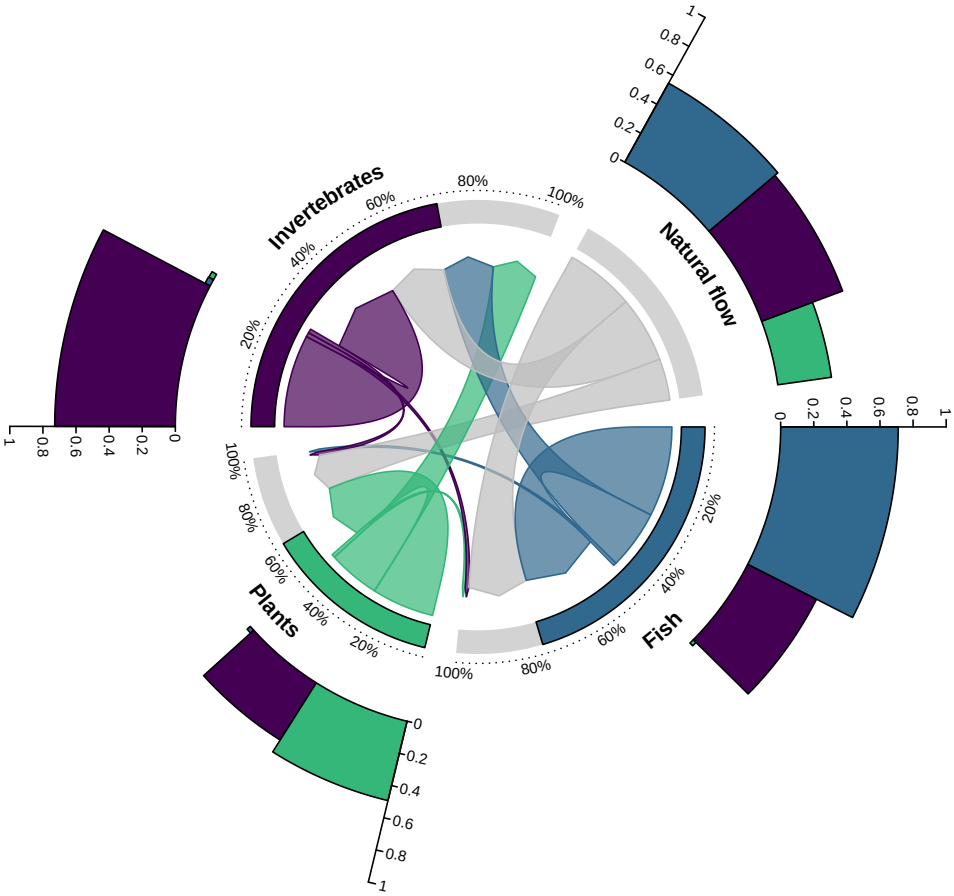

Figure 3: The ecosystem-wide effects of designer and natural flow regimes. Each of the four figure sectors represents a particular flow regime and/or ecosystem component: the natural flow regime and three designer flow regimes (riparian vegetation, fishes, and invertebrates). The effects of designer flow regimes on each component are shown, both targeted (arrow returns to same figure sector; e.g. fish to fish) and non-targeted (arrow from one sector to another; e.g. fish to plants), as well as the natural flow regime. Arrow widths correspond to the relative effects of a particular flow scenario (source of arrow) on all other components (arrow endpoint; larger equal more positive responses). These values are shown as proportions of maximum in the outermost bars (1 = maximum; e.g. native fish biomass 100% of carrying capacity). For instance, when designing flows to most benefit native fishes, fish respond strongly (large arrow and outer bar) but plants perform poorly (small arrow and bar). The bar tracking the circumference of the center arrows represents the difference between the natural and prescribed flow for the group in that sector (given in percentage). For example, under the natural flow regime, fish achieve 77% of the biomass achieved under the designer flow.

JD Tonkin *et al.* – Supporting Information

WebPanel 1. Methods

Target scenarios

Using species common to rivers in the Colorado Basin of the southwestern United States, we defined biodiversity target results that managers may seek to maximize downstream from a large dam for three components of a river-riparian (hereafter "river") ecosystem: cottonwood tree coverage as a percent of reach-wide riparian community carrying capacity, native fish species biomass as a percent of reach-wide fish community carrying capacity, and terrestrially-available benthic invertebrates as a percent of population carrying capacity. Using these targets, coupled with mechanistic population models, we designed flow regimes that maximized the value of the target. We then explored the population- and community-level impacts of these flow regimes on other components of the ecosystem by projecting each flow regime up to 200 years into the future and quantifying the outcome. We also examined a natural flow regime scenario using a hydrograph derived from a large free-flowing river in the southwestern USA (Verde River, Arizona) and quantified the relative differences and tradeoffs across the ecosystem components.

Modeling frameworks

We modeled the three ecosystem components using three independent existing models (Lytle et al., 2017; McMullen et al., 2017; Rogosch et al., 2019). Riparian vegetation and fishes were modeled using a novel application of coupled, stage-structured matrix population models (Lytle et al., 2017; Rogosch et al., 2019). These models link the flow regime directly with population dynamics in a coupled framework that enables an understanding of whole-community dynamics and can incorporate stochasticity by taking random draws from a sequence of river flow year types. The models operate at the reach scale and share a central dependency assumption that represents the whole-community carrying capacity for which the organisms exploitatively compete. A unique attribute of these models is their ability to identify how complex species interactions change under novel environmental conditions, which allowed us to quantify species performance under all possible environmental states (Tonkin et al., 2018). Space (areal extent) in the riparian landscape is the finite element for riparian plants (Lytle et al., 2017), whereas maximum total biomass for each reach is the finite element for fishes (Rogosch et al., 2019). The models employ different methods to realize density dependence, which can be found in the relevant publications (Lytle et al., 2017; Rogosch et al., 2019; McMullen et al., 2017). Floods and droughts interact with vital rates, affecting population

sizes, which opens vacant space or biomass for recruitment during the next year if conditions are met. Both models have demonstrated a strong ability to recover known patterns on the landscape via tests against empirical data (Lytle et al., 2017; Rogosch et al., 2019).

The plant community comprised five taxa with six stage classes from seedling to reproductive adult: cottonwoods (*Populus deltoides*), tamarisk (*Tamarix ramosissima*), willow (*Salix exigua*), meadow grasses, and sagebrush (*Artemisia tridentata*). These taxa are representative of dominant groups across dryland regions. Each taxon j is described by a stage-based matrix $N_j(t+1) = A_j(t)N_j(t)$, where $N_j(t)$ is a vector containing stage abundances and $A_j(t)$ is a set of transition matrices that fluctuate according to variation in the hydrograph (Caswell, 2001). Thus, the population dynamics of each taxa are determined primarily by how their vital rates (stage-specific flood and drought mortality, fecundity, self-thinning) are affected by annual cycles of flooding and drought. Vital rates were sourced from a variety of locations including aerial photograph time-series, literature, experimentation (e.g. Cooper et al., 1999) and field surveys. Detailed definitions of the vital rate parameters and model structure can be found in Lytle et al. (2017). The plant model is fully ergodic, so we ran a single simulation for all scenarios.

The fish community comprised seven species, each with three stage classes, covering a range of body sizes and representing the major life-history tradeoffs among growth, survival, and reproduction (Olden et al., 2006). The community comprised three species native to the southwest USA: desert sucker (*Catostomus clarki*; CACL), Sonora sucker (*Catostomus insignis*; CAIN) and roundtail chub (*Gila robusta*; GIRO); and four non-native species: yellow bullhead (*Ameiurus natalis*; AMNA), green sunfish (*Lepomis cyanellus*; LECY), smallmouth bass (*Micropterus dolomieu*; MIDO), and red shiner (*Cyprinella lutrensis*; CYLU). The model conforms to the same general structure as the plant model, with some minor differences in how the vital rates interact with the hydrograph, details of which can be found in Rogosch et al. (2019). Vital rates, including the addition of the Gonadal-Somatic Index to estimate the proportion of egg biomass produced, were sourced from literature reviews. We used 100 iterations for each model run, starting by sampling initial abundance for each species from a negative binomial distribution populated with means and variances from a long-term empirical dataset (seven sites in the upper Verde River, 1994-2008) (Rogosch et al., 2019).

Benthic invertebrates were modeled using a novel form of the logistic growth model that enables carrying capacity (K) to fluctuate through time (McMullen et al., 2017). Carrying capacity, in this case, responds to flood events. For flood-adapted species, carrying capacity is highest immediately post-flood. The magnitude of a flood pulse determines the magnitude of change in K, and this relationship can be modeled for events of any magnitude and for multiple, repeated events. For flood-averse species, carrying capacity is reduced post-flood and increases with time since flood event. Although the model also allows population growth rate (r) to vary with time, we kept r fixed. Contrary to the fish and riparian plant models,

this model operates on individual populations in that the populations do not share a finite resource such as space or biomass: each population has its own carrying capacity. The details of the model can be found in McMullen et al. (2017).

We modeled three invertebrate taxa: a fast life-cycle, flood-adapted mayfly, *Fallceon* spp. (Ephemeroptera: Baetidae); a slow life-cycle, flood-adapted dragonfly *Progomphus* spp. (Odonata: Gomphidae); and a flood-averse ostracod seed shrimp (Crustacea: Ostracoda). We used the same parameters for each taxon as those in (McMullen et al., 2017). Briefly, K for both mayflies and dragonflies was maximized (100) immediately following floods, and declined to K = 40 (40% of maximum possible) after a period of time (depending on the shape parameter g, which regulates the rate that K returns to pre-disturbance levels). Both taxa favor open riffle and sandy habitats created by disturbance, which is reduced by encroaching vegetation through time in these dryland rivers. By contrast, K for the ostracod reduced to 40 post-disturbance and increased to 100 after a period of baseflow. Floods reduce preferred habitats of ostracods—slow-water habitats, often created by beaver dam impoundments or large amounts of edge vegetation. The mayfly, dragonfly and ostracod differed in their r (mayfly: 0.23; dragonfly: 0.08; ostracod: 0.16) and h (strength of disturbance mortality relationship; mayfly: 0.02; dragonfly: 0.01; ostracod: 0.05). Detailed descriptions can be found in McMullen et al. (2017).

For the sake of simplicity in the invertebrate model, we did not consider in our simulations that 1. there are likely seasonal effects in population dynamics, meaning population growth may be slower during different parts of the year; and 2. with only small floods in our designer flow scenario, other factors such as beaver dam construction, dominance of filamentous green algae, and bed armoring would likely begin to play major roles over time. In this sense, the flows we designed for invertebrates may not be optimal at longer time scales. The major flows that benefit fishes and cottonwoods could be needed for the invertebrates as well to reset the system and reorganize channel and floodplain morphology (Shafroth et al., 2010). Moreover, our modeling does not incorporate negative feedbacks (e.g. low secondary production leading to reduced fish production, despite flow that is tailored towards fishes) that may be present in real-world ecosystems (Anderson et al., 2006). Connecting the three ecosystem components in this way remains an important topic for exploration.

Hydrograph details

Although our approach was simulation-based in a generalized river in the southwestern United States, we used a real flow regime to generate a natural hydrograph vector. To do this, we sourced a 45-year (1964-2008) historical hydrograph from the upper Verde River (U.S. Geographical Survey gauge number 09503700) near Paulden, Arizona. All three groups were modeled from this one central flow regime, enabling a comparison of community dynamics

across the whole ecosystem.

We converted this hydrograph into the format required to inform each of the models. For the plant and fish models, this required converting the continuous time hydrograph into a vector of 'year-types'; the models operate on an annual time-step. These year-types were defined using discharge thresholds for floods and droughts (so the variables are binary). We evaluated the plant and fish simulations by projecting forward 200 years, discarding the first 10 years as burn-in and averaging the remainder of years (see Fig. 1 and 2). Thus, we first extended the 45-year natural hydrograph by repeating the sequence out to 200 years.

The fish model converts the hydrograph into one of six flow year types: high spring flood, medium spring flood, summer flood, spring/summer flood, drought, and non-event. Having both high spring flood and summer flood occur in one year was a possibility in this model, but all other year types were mutually exclusive. High spring flood events are those that overtop the banks (greater than 19.8 m^3s^{-1}, a 4-year return interval), whereas medium spring floods correspond to bankfull events (6.2 m^3s^{-1}, 2.5-year return interval). Monsoon season summer floods are roughly equivalent in magnitude to medium spring-flood events. Drought years represent years without floods and with sustained (at least 40 days) low-flow conditions. Non-event years are those that do not meet any of these criteria.

The plant model operates with three independent year types: flood, drought and non-event years. Flood years correspond to the spring high flood years in the fish model, thus representing large bank over-topping floods during the spring recruitment window for cottonwood and tamarisk; "recruitment box model" (Mahoney and Rood, 1998). Likewise, drought years correspond to drought years in the fish model. Non-event years here represent years that are not flood or drought years, thus differing from non-event years in the fish model, since the plant model does not consider medium spring floods or summer floods.

Finally, because the invertebrate model is a continuous-time model that incorporates multiple flood events within a single year, generating a natural flow vector required a different approach than the other models. Broadly, we placed natural flow events into seasonal categories, where the peaks typically occur in these arid southwest USA rivers, to achieve compatibility with the riparian and fish models. First, we took the full historical hydrograph from the Verde River and calculated the mean maximum values for each month across the full sequence to identify seasonal flow peaks. We then identified the seasonal window in which these peaks occurred as they vary annually: spring (larger peak) and late summer/fall monsoon season (smaller peak). We then used this window to search for each of the two peaks, taking the mean maximum flow found in these windows across the full 45-year hydrograph. These two flood pulses represent a single year of the natural flow for the invertebrate model. We repeated this same single year for 30 years to run as the natural flow regime for the invertebrates. We evaluated the invertebrates by projecting forward 30 years, discarding the first

10 years as 'burn-in', and averaging the final 20 years (See Fig. 3).

Flow design

We searched a large amount of alternative parameter space to find the optimal sequence of flow events for each target. For riparian plants and fishes, flow design followed a series of steps that incrementally adjusted the frequency of particular year-types. For riparian plants, we adjusted the frequency of flood, drought and non-event years until our target (cottonwood percent of K) was maximized. This step required us to evaluate community dynamics under a range of flow regimes (sequences and combinations of year-types). The resulting prescribed flow regime consisted of a spring flood every six years, preceded by a drought year, with a series of non-event years in between (WebTable 1). These floods occurred within the spring window that enabled cottonwood and tamarisk to recruit. Similar results were produced for cottonwoods at frequencies from 2 to 6-year flood return interval. Adding droughts decreases willow, and these drought years were most effective immediately preceding flood years; post-flood drought increased mortality of newly-recruited cottonwood seedlings as drought mortality decreases with life stage.

For fishes, we adjusted the frequency of spring and summer floods, droughts and non-event years. The fish model also has the option for a medium flood in the spring window, but we only focused on large bank-topping floods, which are consistent with the riparian model's spring floods. The resulting prescribed flow regime for native fish percentage consisted of a spring flood every year. Similar to riparian vegetation, multiple settings produced similar results, but annual floods were optimal.

In contrast to the plant and fish models, the invertebrate model operates in real time and the three taxa do not interact. Each species has its own carrying capacity, which we scaled to 100. Our target was maximizing the terrestrially available taxa: a dragonfly and a mayfly. To do this, we sought to maximize the average value of these two (i.e. % of K) over the 20-year evaluation period. To ensure realism in the allocation of water for the invertebrate prescription, we constrained the maximum number of pulses per year to be four. We sequentially ran through scenarios with a frequency of flood pulses ranging from four per year to one every two years and in magnitude from 2.4 to 80.9 m^3s^{-1}. The resulting scenario that maximized the target was four small pulses (4 m^3s^{-1}) per year, below the threshold of a flood in either the fish or riparian models. Therefore, invertebrate prescription results in 100% of years being non-event years for the non-target taxa. The plant- and fish-prescribed models were converted into m^3s^{-1} for the invertebrate model, based on the threshold used to set floods. This resulted in one large flood (19.8 m^3s^{-1}) every 2,190 days for the plant prescription and one every 365 days for the fish prescription.

Evaluation of model simulations

All model runs were evaluated by discarding the initial ten-year projection as burn-in and averaging the remaining years in each projection: final 20 years of a 30-year projection for invertebrates, final 190 years of a 200-year projection for fish and plants. These values were used to quantify the tradeoff values that went into Fig. 3. All analyses were performed in R 3.3.3 (R Core Team, 2017).

JD Tonkin *et al.* – Supporting Information

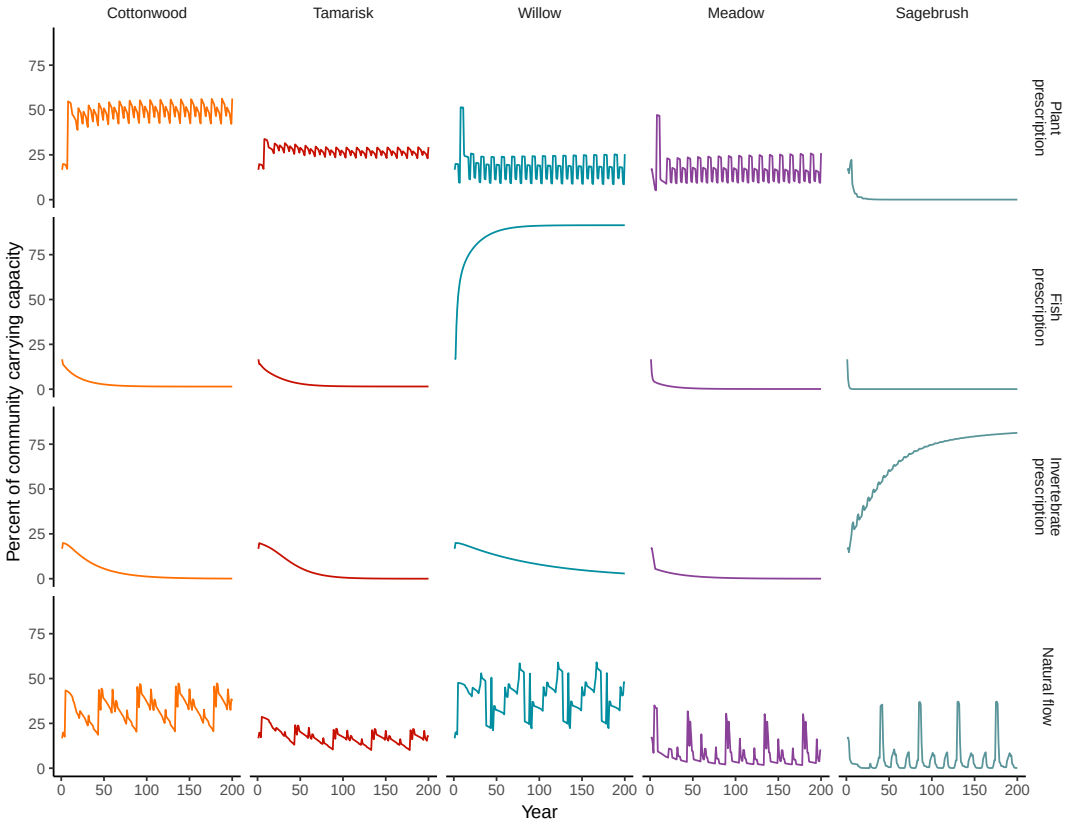

WebFigure 1: Results of simulations for the five riparian plant taxa and four flow scenarios. Maximum cottonwood percentage was the flow target.

JD Tonkin *et al.* – Supporting Information

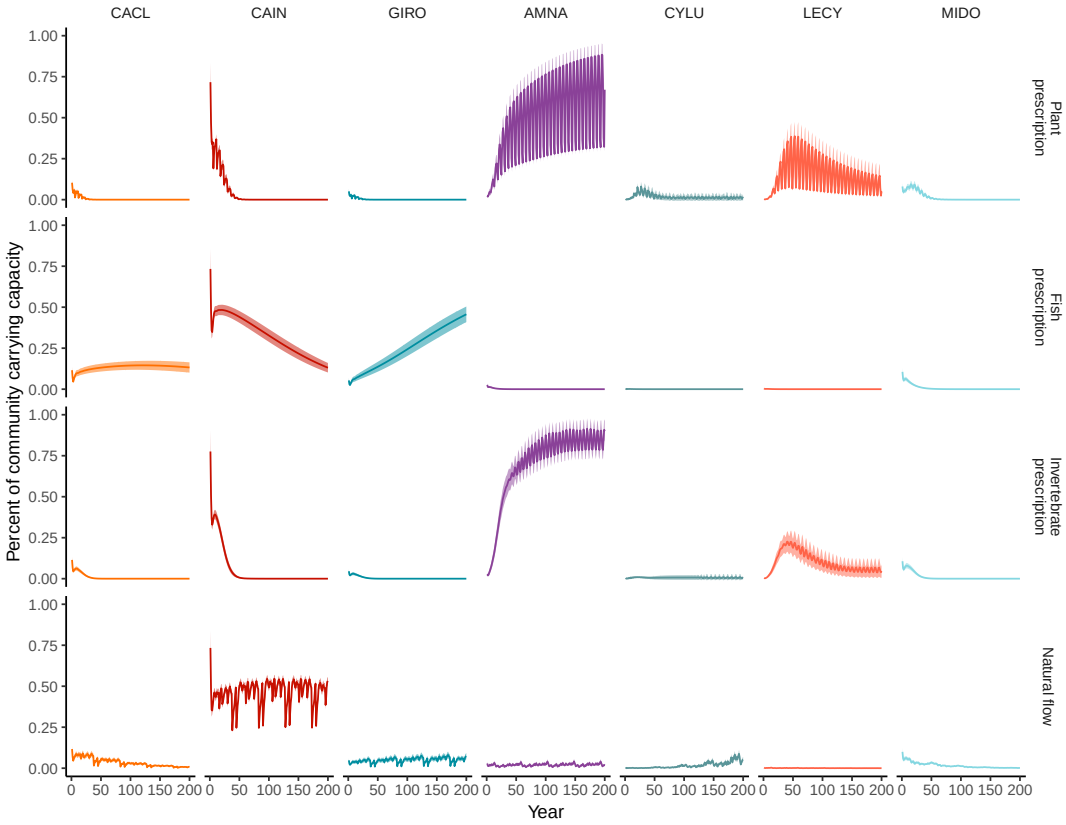

WebFigure 2: Results of simulations for the seven fish species and four flow scenarios. The flow target was maximum percent of the three native species to the southwest USA combined: desert sucker (*Catostomus clarki*; CACL), Sonora sucker (*Catostomus insignis*; CAIN) and roundtail chub (*Gila robusta*; GIRO). The four non-native species were: yellow bullhead (*Ameiurus natalis*; AMNA), green sunfish (*Lepomis cyanellus*; LECY), smallmouth bass (*Micropterus dolomieu*; MIDO), and red shiner (*Cyprinella lutrensis*; CYLU). The line represents the mean of 100 iterations and the band around the line represents 2 standard errors.

JD Tonkin *et al.* – Supporting Information

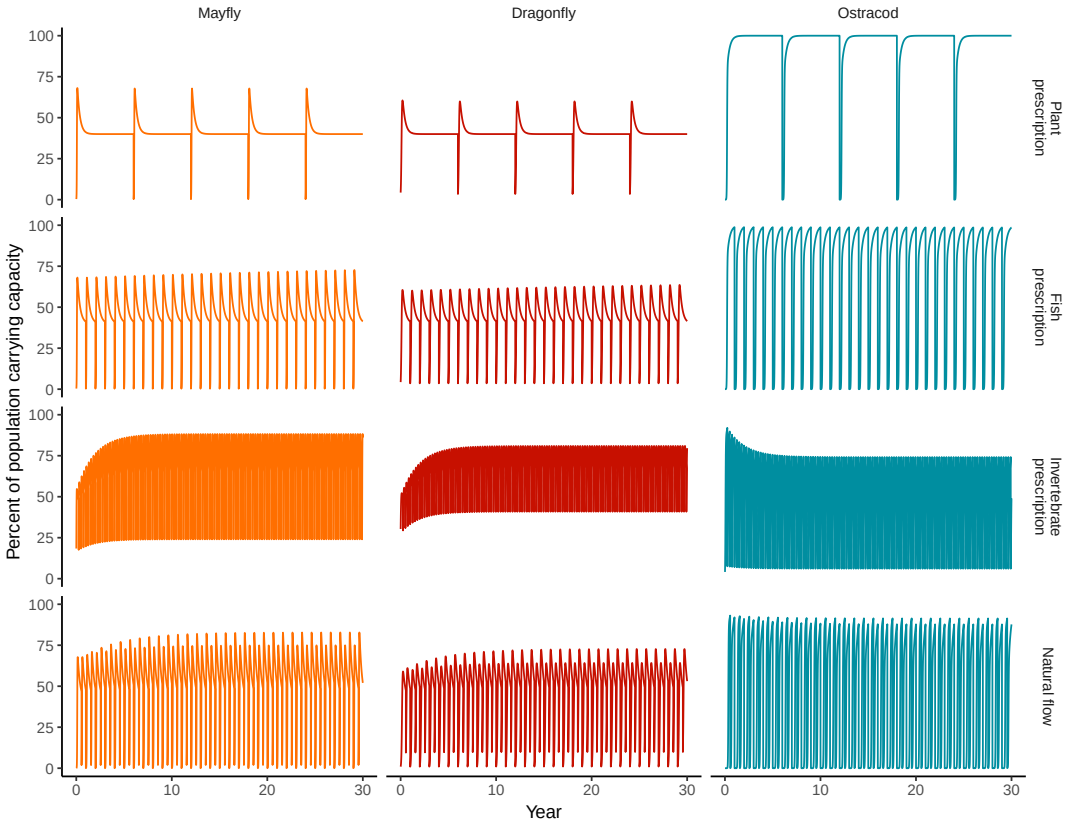

WebFigure 3: Results of simulations for the three invertebrate taxa and four flow scenarios. Maximum mean percent of population carrying capacity for the mayfly and dragonfly was the flow target.

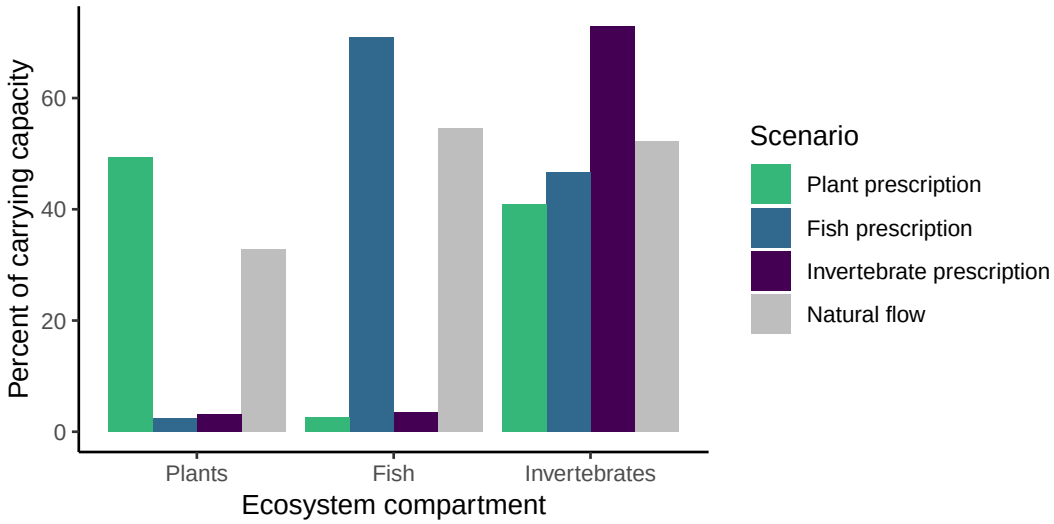

WebFigure 4: Results of simulations for target and non-target ecosystem components. These values were used to create the chord diagram in the main text.

JD Tonkin *et al.* – Supporting Information

WebTable 1: Summary of the models used, the final designer flow for each ecosystem component, and the magnitude of the high-flow pulses.

Group	Model	Flow	Magnitude (m^3s^{-1})
Vegetation	Coupled matrix pop. model	6-y return on large spring floods, preceded by 1 drought and 4 non-event years	19.8
Fish	Coupled matrix pop. model	1 large spring flood every year	19.8
Invertebrates	Time-varying logistic model	4 small pulses per year	4.0